

## Cell-Permeable Peptide Nucleic Acid Designed to Bind to the 5'-Untranslated Region of E-cadherin Transcript Induces Potent and Sequence-Specific Antisense Effects

Anca Dragulescu-Andrasi,<sup>†</sup> Srinivas Rapireddy,<sup>†</sup> Gaofei He,<sup>†</sup>  
Birendra Bhattacharya,<sup>‡</sup> Jens J. Hyldig-Nielsen,<sup>‡</sup> Gerald Zon,<sup>‡</sup> and Danith H. Ly<sup>\*†</sup>

Contribution from the Department of Chemistry, Carnegie Mellon University, 4400 Fifth Avenue, Pittsburgh, Pennsylvania 15213, and Applied Biosystems, 850 Lincoln Centre Drive, Foster City, California 94404

Received May 15, 2006; E-mail: dly@andrew.cmu.edu

**Abstract:** Establishing a general and effective method for regulating gene expression in mammalian systems is important for many aspects of biological and biomedical research. Herein we report the antisense activities of a cell-permeable, guanidine-based peptide nucleic acid (PNA) called GPNA. We show that a GPNA oligomer designed to bind to the transcriptional start-site of human E-cadherin gene induces potent and sequence-specific antisense effects and is less toxic to the cells than the corresponding PNA–polyarginine conjugate. GPNA confers its silencing effect by blocking protein translation. The findings reported in this study provide a molecular framework for designing the next generation cell-permeable nucleic acid mimics for regulating gene expression in live cells and intact organisms.

### Introduction

With the completion of the Human Genome Project, where the human genome and the genomes of many biomedically relevant organisms have been completely sequenced,<sup>1–3</sup> researchers are now faced with the daunting task of making sense of this massive collection of sequence information.<sup>4</sup> The human genome alone has more than 25 000 genes, and only a small fraction of these genes have had their functions determined.<sup>5,6</sup> An important goal in the postgenomics era is to determine what the rest of these genes do and how they are regulated, in normal development as well as in a diseased state. Understanding the precise functional and regulatory roles of these genes is crucial to understanding the pathology of and to developing effective means for treating and detecting genetic diseases.<sup>7,8</sup> To achieve this goal in a reasonable time will require the development of an effective (and ideally high-throughput) strategy for regulating gene expression in live cells and intact organisms.

Several strategies have been developed to regulate gene expression,<sup>9–14</sup> but very few take full advantage of the sequence

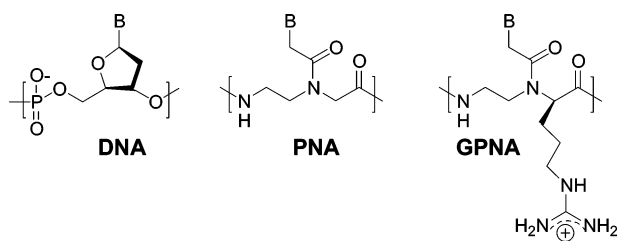
information. One such strategy is antisense.<sup>15</sup> Antisense could potentially be a powerful technology for controlling gene expression, because it relies on the simple rules of Watson–Crick base-pairing for recognition and the general notion that all gene products (proteins) are made in accordance with the central dogma of molecular biology—in that the genetic information encoded in double helical (genomic) DNA is first transcribed into messenger RNA (mRNA) as a carrier molecule before it is translated into protein.<sup>16,17</sup> With the sequence of many genes and gene transcripts annotated,<sup>3</sup> it should, in principle, be possible to regulate the expression of any genes simply by designing oligonucleotides to bind to the corresponding gene transcript. Such binding would either activate the RNase H-dependent cleavage of the RNA targets or directly block protein translation, depending on the type of the oligonucleotides used.<sup>18</sup> Either way, such binding would lead to selective gene silencing.

Though simple in theory, antisense has proven rather challenging in execution.<sup>19</sup> Many researchers are now beginning to question this technology, due to the unresolved issues with oligonucleotide design,<sup>20,21</sup> cellular delivery,<sup>22,23</sup> and off-target

<sup>†</sup> Carnegie Mellon University.

<sup>‡</sup> Applied Biosystems.

- (1) Lander, E. S.; et al. *Nature* **2001**, *409*, 860–921.
- (2) Venter, C.; et al. *Science* **2001**, *291*, 1304–1351.
- (3) Ensembl Genome Browser: [www.ensembl.org/index.html](http://www.ensembl.org/index.html).
- (4) Galas, D. J. *Science* **2001**, *291*, 1257–1260.
- (5) Ewing, B.; Green, P. *Nat. Genet.* **2000**, *25*, 232–234.
- (6) Crollius, H. R.; Jaillon, O.; Bernot, A.; Dasilva, C.; Bouneau, L.; Fischer, C.; Fizames, C.; Wincker, P.; Brottier, P.; Quetier, F.; Saurin, W.; Weissenbach, J. *Nat. Genet.* **2000**, *25*, 235–238.
- (7) Jimenez-Sanchez, G.; Childs, B.; Valle, D. *Nature* **2001**, *409*, 853–855.
- (8) Peltonen, L.; McKusick, V. A. *Science* **2001**, *291*, 1224–1229.
- (9) Stockwell, B. R. *Nat. Rev. Genet.* **2000**, *1*, 116–125.
- (10) Scherer, L. J.; Rossi, J. J. *Nat. Biotechnol.* **2003**, *21*, 1457–1465.
- (11) Dervan, P. B.; Poulin-Kerstien, A. T.; Fechter, E. J.; Edelson, B. S. *Top. Curr. Chem.* **2005**, *253*, 1–31.
- (12) Jantz, D.; Amann, B. T.; Gatto, G. J.; Berg, J. M. *Chem. Rev.* **2004**, *104*, 789–800.
- (13) Faria, M.; Giovannangeli, C. *J. Gene Med.* **2001**, *3*, 299–310.
- (14) Nielsen, P. E. *Acc. Chem. Res.* **1999**, *32*, 624–630.
- (15) Mesmaeker, A.; Haner, R.; Martin, P.; Moser, H. E. *Acc. Chem. Res.* **1995**, *28*, 366–374.
- (16) Dove, A. *Nat. Biotechnol.* **2002**, *20*, 121–124.
- (17) Tamm, I.; Dorken, B.; Hartmann, G. *Lancet* **2001**, *358*, 489.
- (18) Milligan, J. F.; Matteucci, M. D.; Martin, J. C. *J. Med. Chem.* **1993**, *36*, 1923–1937.
- (19) Stein, C. A. *Nat. Biotechnol.* **1999**, *17*, 209–209.
- (20) Smith, L. M.; Andersen, K. B.; Hovgaard, L.; Jaroszewski, J. W. *Eur. J. Pharm. Sci.* **2000**, *11*, 191–198.
- (21) Tu, G.-c.; Cao, Q. n.; Zhou, F.; Israel, Y. *J. Biol. Chem.* **1998**, *273*, 25125–25131.

**Scheme 1.** Chemical Structure of DNA, PNA, and GPNA Unit

and cytotoxic effects.<sup>19,24</sup> The first issue deals with the difficulty in designing oligonucleotides that would elicit a potent antisense effect. This issue has been attributed in part to the complex secondary and tertiary structures of RNA, which are difficult to predict a priori, that hinder oligonucleotides from binding to the intended RNA targets. The second issue concerns cellular delivery; specifically, how to get nucleic acids (and their synthetic mimics) across the lipid bilayers of the cell membrane. Most oligonucleotides are not cell-permeable, and their delivery into cells would require the assistance of either transfecting reagents or mechanical or electrical transduction. Oligonucleotides, delivered with the aid of transfecting reagents, are generally trapped in the vesicles and degraded or recycled back to the cell surface before escaping to the cytoplasm and to the nucleus,<sup>22</sup> while those delivered with the aid of mechanical or electrical transduction are generally limited to small-scale experimental setups. The third issue concerns nonspecific binding and cytotoxic effects. The insufficient antisense effect commonly found in antisense studies prompts researchers to increase the dosage so that a desired effect can be attained. Increasing the reagent dosage would lead to off-target and cytotoxic effects. These latter effects, in fact, have been suggested as the primary source of unreliability in many published studies.<sup>19</sup> The ability to design antisense reagents that can overcome these long-standing challenges will have a broad impact on the future role of this technology in biology and medicine.

An important class of antisense (and antigene) molecules developed in the past decade is peptide nucleic acid (PNA).<sup>14,25</sup> PNA is a synthetic analogue of DNA and RNA, developed more than a decade ago, in which the naturally occurring sugar-phosphate backbone has been replaced by *N*-(2-aminoethyl) glycine units (Scheme 1). PNA can hybridize to complementary DNA or RNA strand through Watson-Crick base-pairing to form a hybrid duplex, with high affinity and sequence selectivity.<sup>26</sup> The high binding affinity of PNA has been attributed in part to the lack of electrostatic repulsion.<sup>27</sup> In addition to conferring hybridization stability, the neutral polyamide backbone provides the added benefit of enzymatic stability, making PNA resistant to both proteases and nucleases.<sup>28</sup> Together these properties make PNA an attractive reagent for biotechnology

applications.<sup>29,30</sup> Despite the impressive progress that has been made in the past decade, the goal of using PNA for in vivo applications has not yet been fully realized; for the most part, this can be attributed to the poor cellular uptake properties of PNA.<sup>31</sup> This inherent limitation has prevented PNA from finding widespread biomedical applications.

Recognizing the importance of PNA in biology and medicine, we have recently initiated a research program to explore the structure of PNA in an attempt to improve its intrinsic cellular uptake properties.<sup>32</sup> Recently we showed that GPNA, an analogue of PNA containing internally linked *D*-arginine side chains, binds to RNA with high affinity and sequence selectivity and is readily taken up by mammalian cells.<sup>33</sup> Although promising, the ability of GPNAs to inhibit gene expression has not yet been addressed. Herein we show that GPNA designed to bind to the transcriptional start-site of E-cadherin gene induces potent and sequence-specific antisense effects and is less toxic to the cells than the corresponding PNA-polyarginine conjugate. The results reported in this study have important implications on the future design of cell-permeable nucleic acid mimics for regulating gene expression in live cells and intact organisms.

## Results and Discussion

**Target Selection and Oligonucleotide Design.** As a model system, we had selected E-cadherin as a gene target. E-cadherin is a transmembrane glycoprotein that mediates Ca<sup>2+</sup>-dependent cell-cell adhesion (Figure 1).<sup>34-36</sup> It is highly expressed in most adherent cells and localized at the periphery of the cell membrane. These properties make E-cadherin an attractive target for antisense study, because the protein expression level could be rapidly assessed with immunofluorescent chemistry. Since E-cadherin is an intercellular adhesion molecule, downregulation of this gene would lead to a loss in cell-cell contact inhibition and an increase in cell motility,<sup>35</sup> both of which can be easily assessed by monitoring changes in cell morphology and motility. In addition to mediating homodimerization, the intracellular domain of E-cadherin interacts with  $\beta$ -catenin, an important component of the canonical Wnt signaling pathway.<sup>35</sup> In the absence of Wnt signaling,  $\beta$ -catenin is sequestered by E-cadherin and those that remain in the cytoplasm are tagged for degradation by the Axin-APC-GSK-3 $\beta$  protein complex. Under circumstances in which E-cadherin is downregulated or functionally inactivated or Wnt signaling is turned on,  $\beta$ -catenin is accumulated in the cytoplasm and subsequently translocated to the nucleus, where it transactivates a series of genes involved in key cell cycle regulation and maintenance (Figure 1). Targeting E-cadherin would, therefore, not only allow one to assess antisense effects at the transcriptional and translational level, but also evaluate the downstream molecular and cellular phenotypes, which is important for antisense studies, since many antisense reagents are toxic to the cells, especially at moderate concentrations.

(22) Juliano, R. J.; Yoon, H. *Curr. Opin. Mol. Ther.* **2000**, *2*, 297-303.

(23) Lebedeva, I.; Benimetskaya, L.; Stein, C. A.; Vilenchik, M. *Eur. J. Pharm. Biopharm.* **2000**, *50*, 101-119.

(24) Monia, B. P. *Nat. Med.* **1999**, *5*, 127.

(25) Nielsen, P. E.; Egholm, M.; Berg, R. H.; Buchardt, O. *Science* **1991**, *254*, 1497-1500.

(26) Egholm, M.; Buchardt, O.; Christensen, L.; Behrens, C.; Freier, S. M.; Driver, D. A.; Berg, R. H.; Kim, S. K.; Norden, B.; Nielsen, P. E. *Nature* **1993**, *365*, 566-568.

(27) Tomac, S.; Sarkar, M.; Ratilainen, T.; Wittung, P.; Nielsen, P. E.; Norden, B.; Graeslund, A. *J. Am. Chem. Soc.* **1996**, *118*, 5544-5552.

(28) Gambacorti-Passerini, C.; Mologni, L.; Bertazzoli, C.; LeCoutre, P.; Marchesi, E.; Grignani, F.; Nielsen, P. E. *Blood* **1996**, *88*, 1411-1417.

(29) Nielsen, P. E. *Curr. Opin. Biotechnol.* **1999**, *10*, 71-75.

(30) Nielsen, P. E. *Mol. Biotechnol.* **2004**, *26*, 233-248.

(31) Koppellhus, U.; Nielsen, P. E. *Adv. Drug Delivery Rev.* **2003**, *55*, 267-280.

(32) Zhou, P.; Wang, M.; Du, L.; Fisher, G. W.; Waggoner, A.; Ly, D. H. *J. Am. Chem. Soc.* **2003**, *125*, 6878-6879.

(33) Dragulescu-Andrasi, A.; Zhou, P.; He, G.; Ly, D. H. *Chem. Commun.* **2005**, 244-246.

(34) Tepass, U.; Truong, K.; Godt, D.; Ikura, M.; Peifer, M. *Nat. Rev. Mol. Cell Biol.* **2000**, *1*, 91-100.

(35) Nelson, W. J.; Nusse, R. *Science* **2004**, *303*, 1483-1487.

(36) Moon, R. T.; Bowerman, B.; Boutros, M.; Perrimon, N. *Science* **2002**, *296*, 1644-1646.

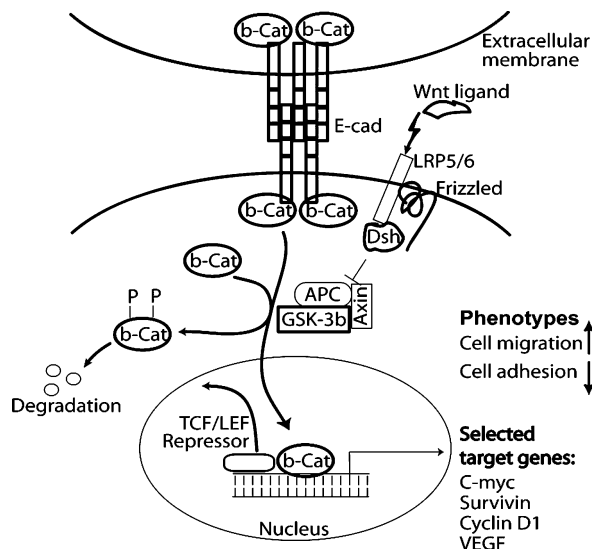
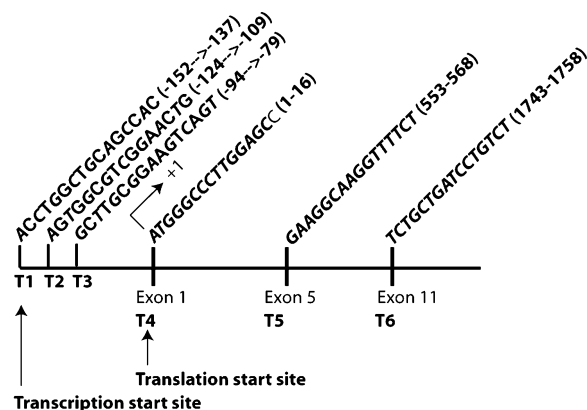


**Figure 1.** The role of E-cadherin in  $\text{Ca}^{2+}$ -mediated cell adhesion. E-Cadherin is localized at the periphery of the cell membrane.  $\beta$ -Catenin binds to the intracellular domain of E-cadherin, protecting it from phosphorylation and degradation. When E-cadherin is downregulated (or functionally inactivated) or Wnt signaling pathway is turned on,  $\beta$ -catenin is accumulated in the cytoplasm and subsequently translocated to the nucleus, where it activates the transcription of a series of genes.

**Scheme 2.** Human E-cadherin Gene Transcript and the Sequence of GPNA Oligomers Designed To Bind to the Corresponding Regions<sup>a</sup>



**T1:** H-GTGGCTGCAGCCAGGT-NH<sub>2</sub>

**T2:** H-CAGTTCGACGCCACT-NH<sub>2</sub>

**T3:** H-ACTGACTTCCGCAAGC-NH<sub>2</sub>

**T4:** H-GGCTCCAAGGGCCCAT-NH<sub>2</sub>

**T5:** H-CTGGCAGAGCCAAGAG-NH<sub>2</sub>

**T6:** H-AGAAAACCTTGCCTTC-NH<sub>2</sub>

<sup>a</sup> The nucleobases written in bold letters contain *N*-(2-aminoethyl)-*D*-arginine backbone units (GPNA units).

Scheme 2 shows the structure of the E-cadherin transcript, along with the various regions to which GPNA oligomers were designed to bind. A total of six regions, including the transcriptional (T1) and translational (T4) start-site, were selected, and the complementary GPNA oligomers were designed. It should be noted that the public databases Ensembl Genome Browser,

NCBI, RefSeq, and Transcriptional Start Sites all list T2 as the transcriptional start-site for E-cadherin, but a recent study revealed that the actual transcriptional start-site is further upstream than what is indicated in these databases.<sup>37</sup> This start-site corresponds to the region shown in T1 (Scheme 2). This discrepancy highlights the need to validate the transcriptional start-sites taken from these databases before they could reliably be incorporated into the antisense (and antigene) design.

GPNA oligomers (T1–T6) were designed such that the unmodified PNA [*N*-(2-aminoethyl)glycine] and arginine-derived GPNA [*N*-(2-aminoethyl)-*D*-arginine] backbone units were alternated at every other position. This particular design was selected because it provides GPNA with optimal hybridization and cellular uptake properties.<sup>33</sup> The oligomers were synthesized according to established protocols,<sup>38</sup> purified, and characterized by reversed-phase HPLC and MALDI-TOF, respectively.

**Antisense Effects.** To determine the antisense activities of GPNAs, we compared the immunofluorescent-staining of E-cadherin of the treated and untreated cells. The experiment was performed by first seeding the human lung adenocarcinoma (A549) cells on glass coverslips at ~70% density. The next day cells were thoroughly washed with PBS, refreshed with complete media (10% FBS), and then treated with 10  $\mu\text{M}$  of each GPNA oligomer for 72 h. Following a series of processing steps (Figure 2A), cells were stained with E-cadherin primary antibody, counterstained with FITC-labeled secondary antibody, and then imaged with a fluorescence microscope. The fluorescent images of both the untreated and treated cells are shown in Figure 2. The identity of each oligomer is designated in parentheses.

Of the six GPNA oligomers examined, only T1 and T4, which were designed to bind to the transcriptional and translational start-site, respectively, showed antisense effects, as reflected in the changes in the fluorescent intensity and staining pattern. The untreated cells (Figure 2B) showed a strong fluorescent intensity with the “grid” pattern characteristic of the E-cadherin staining.<sup>39</sup> Cells treated with T1 (Figure 2C) and T4 (Figure 2F), on the other hand, showed a significant reduction in the fluorescent intensity, indicating a reduction in the E-cadherin protein level. In addition, these cells exhibited distinct cell morphology, characterized by the elongated cell shape and apparent cell–cell detachment. These characteristic features are consistent with the phenotypes of E-cadherin downregulation.<sup>40</sup> A closer examination of the E-cadherin expression level, inferred from the fluorescent intensity and staining pattern, revealed that while both oligos induced antisense effect, T1 was more potent than T4. No noticeable difference in either the fluorescent intensity or staining pattern was observed for T2, T3, T5, or T6 as compared to the control (compare parts D, E, G, and H with B, Figure 2). This result is consistent with a recent finding by Doyle and Corey,<sup>41</sup> which

(37) Hashimoto, S. i.; Suzuki, Y.; Kasai, Y.; Morohoshi, K.; Yamada, T.; Sese, J.; Morishita, S.; Sugano, S.; Matsushima, K. *Nat. Biotechnol.* **2004**, *22*, 1146–1149.

(38) Christensen, L.; Fitzpatrick, R.; Gildea, B.; Petersen, K. H.; Hansen, H. F.; Koch, T.; Egholm, M.; Buchardt, O.; Nielsen, P. E.; Coull, J. *J. Pept. Sci.* **1995**, *1*, 175–183.

(39) Orsulic, S.; Huber, O.; Aberle, H.; Arnold, S.; Kemler, R. *J. Cell Sci.* **1999**, *112*, 1237–1245.

(40) Cano, A.; Perez-Moreno, M.; Rodrigo, I.; Locascio, A.; Blanco, M. J.; Barrio, M. G. d.; Prottilo, F.; Nieto, M. A. *Nat. Cell Biol.* **2000**, *2*, 76–83.

(41) Doyle, D. F.; Braasch, D. A.; Simmons, C. G.; Janowski, B. A.; Corey, D. R. *Biochemistry* **2001**, *40*, 53–64.

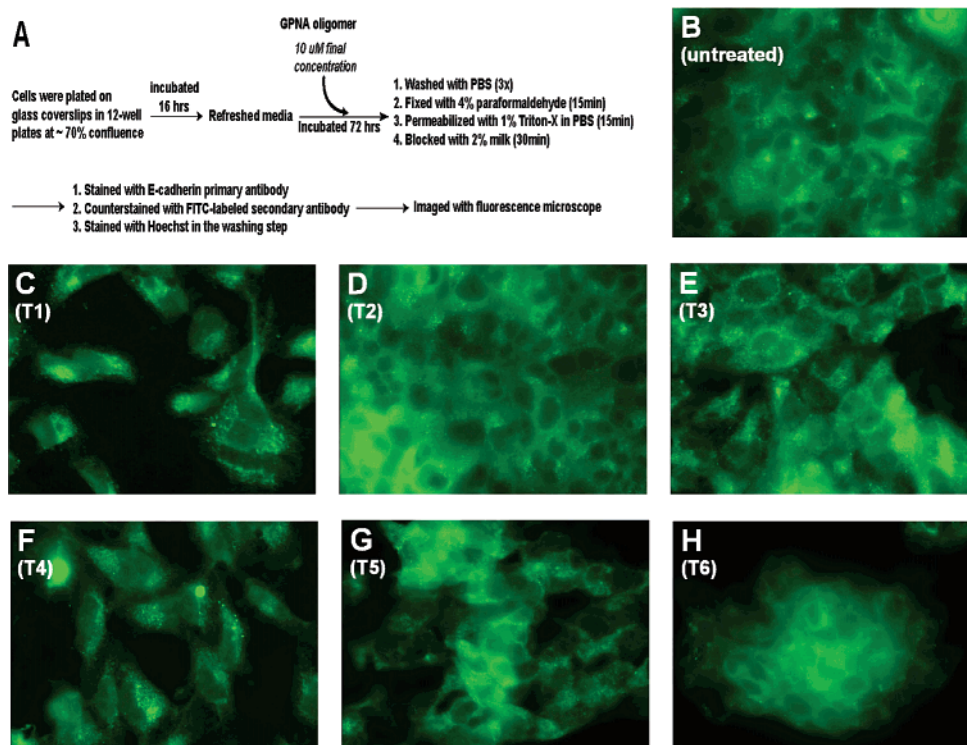


**Figure 2.** E-Cadherin immunofluorescent-staining of the untreated (B) and treated cells (C–H). A549 cells were treated with 10  $\mu\text{M}$  of GPNA for 72 h and then stained with E-cadherin primary antibody and counterstained with FITC-labeled secondary antibody. The identity of each oligomer is indicated in the parentheses. Note that in panel H only a small cell colony is shown. Nevertheless, these cells displayed the characteristic immunostaining profile (pattern and intensity) as that shown in panels B, D, E, and G.

showed that, of the 21 PNA oligomers designed to bind to various regions of the luciferase gene transcript, only one that was designed to bind to the transcriptional start-site induced a potent antisense effect. It is not clearly understood why targeting the transcriptional start-site would yield greater antisense effect than targeting other parts of the gene transcript. One possible explanation could be that the transcriptional start-site is more accessible to GPNA binding than other parts of the transcript. Another plausible explanation could be that targeting this site prevents the binding and proper assembly of the ribosomal machinery, which is likely to be more effective in inhibiting protein translation than simply blocking the translational apparatus from moving forward while it is already on the tract and in a processive mode. This regional effect has been previously documented with PNA<sup>41</sup> and 2'-modified RNA.<sup>42</sup>

**Sequence Specificity.** Next we assessed the sequence specificity of GPNAs by comparing E-cadherin staining of cells treated with perfectly matched (T1) and mismatched (T1-M3) GPNA oligomer. Comparison of parts A–C of Figure 3 reveals that cells treated with T1 had a dramatic reduction in the E-cadherin staining (green) as compared to that of the control or to cells treated with T1-M3. The residual E-cadherin staining seen in Figure 3B could be attributed to the remnant of the old protein produced prior to the treatment, since E-cadherin protein has a relatively long half-life (5 h on the cell surface).<sup>43</sup> On the other hand, comparing cells treated with T1-M3 versus the control shows that they have similar E-cadherin staining intensity, indicating that T1-M3 had no effect on the E-cadherin

expression level, though the staining pattern appears to be somewhat different between the two cell populations. Cells treated with T1-M3 show a more diffused E-cadherin staining pattern as compared to that of the control, which display the prototypical “grid” staining pattern characteristic of E-cadherin localizing at the cell surface.<sup>40</sup> The difference in the staining pattern and in cell size, which appears to be larger for the T1-M3-treated cells (Figure 3C,F,I) as compared to the control (Figure 3A,D,G) and T1-treated cells (Figure 2B,E,H), can be explained in term of cells in a different phase of the cell cycle. Cells used in the T1-M3 treatment were initially seeded at a much lower density than those in the control and in the T1 treatment, which were confluent at the time of immunostaining. Cells used in the T1-M3 treatment, on the other hand, were still in the exponential-growth phase. Actively dividing cells are generally larger in size than the confluent cells, with E-cadherin localized more predominantly in the cytoplasmic compartment than at the adherent junctions.<sup>44,45</sup> In the exponentially dividing cells, a large proportion of E-cadherin protein is in the vesicles trafficking to and from the cell surface. The mechanism by which this occurs is not clearly understood but appears to be autoregulated by cell–cell contact. Despite the subtle differences in E-cadherin staining pattern and cell size, our results showed that only the perfectly matched T1 GPNA can inhibit E-cadherin expression, suggesting that the observed antisense effect is sequence-specific. We have also examined the effects of concentration on the antisense activity of T1 (Supporting Information, Figure S1). A reduction in E-cadherin level was observed at concentrations as low as 1  $\mu\text{M}$ , but less

(42) Baker, B. F.; Lot, S. S.; Condon, T. P.; Cheng-Flournoy, S.; Lesnik, E. A.; Sasmor, H. M.; Bennett, C. F. *J. Biol. Chem.* **1997**, *272*, 11994–12000.  
(43) Jamal, S.; Schneider, R. *J. Clin. Invest.* **2002**, *110*, 443–452.

(44) Angres, B.; Barth, A.; Nelson, W. *J. Cell Biol.* **1996**, *134*, 549–557.  
(45) Yap, A. S.; Brieher, W. M.; Pruschy, M.; Bumbiner, B. M. *Curr. Biol.* **1997**, *7*, 308–315.

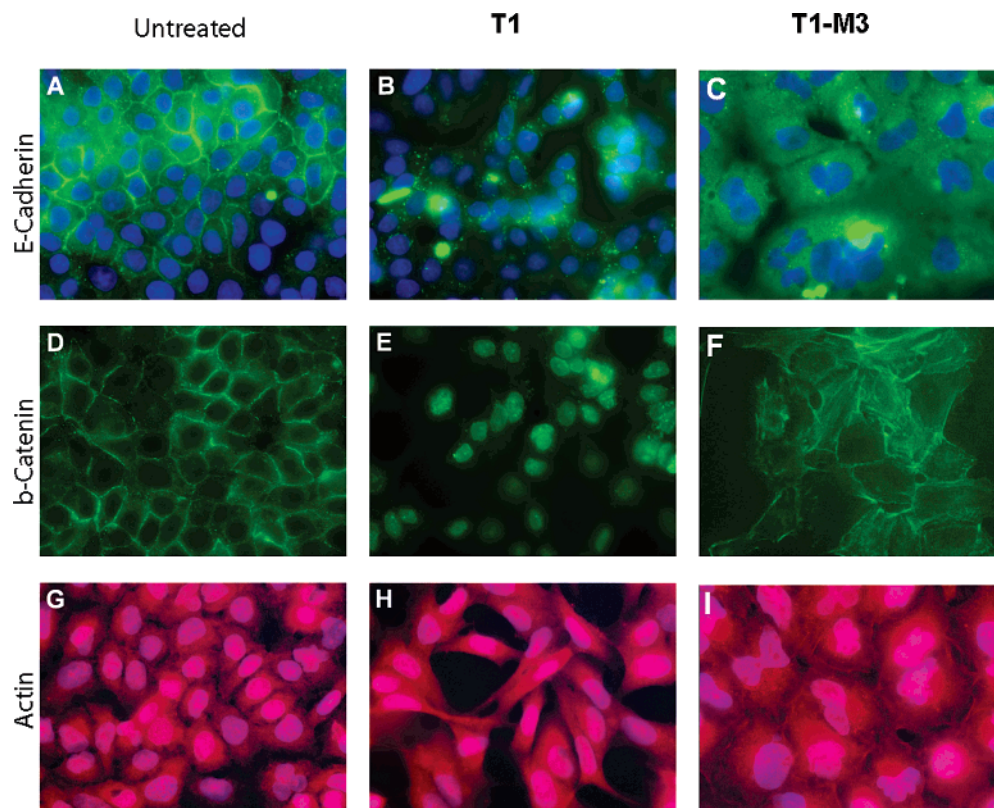


**Figure 3.** Immunostaining of the untreated A549 cells (A, D, G) and cells treated with 10  $\mu\text{M}$  of the perfectly matched **T1** (B, E, H) and mismatched **T1-M3** (C, F, I) GPNA oligomer for 72 h. (A–C) Cells stained with E-cadherin primary antibody and counterstained with FITC-labeled secondary antibody (green) and Hoechst (blue, nucleus). (D–F) Cells stained with  $\beta$ -catenin primary antibody and counterstained with FITC-labeled secondary antibody. Note that Hoechst was not added. (G–I) Cells stained with rhodamine-labeled phalloidin (actin, red) and Hoechst (blue, nucleus). The sequence for **T1-M3**: H-GTGACTGCAACCAAGT-NH<sub>2</sub> (mismatched sites are italic). Note that cells in C, F, and I were in exponential growth-phase, while those in A, B, D, E, G, and H were confluent.

significant than that at 10  $\mu\text{M}$ . The antisense activity of **T1** does not appear to be cell-type specific, since similar results were observed with other cell lines (Supporting Information, Figure S2).

In addition to E-cadherin repression, the **T1**-treated cells, when stained with  $\beta$ -catenin primary antibody and counterstained with FITC-labeled secondary antibody, showed specific nuclear localization (Figure 3E). The untreated and **T1-M3**-treated cells, on the other hand, showed cell-surface staining pattern similar to that of E-cadherin (Figure 3D,F). The two staining patterns are similar because  $\beta$ -catenin and E-cadherin bind to one another. In the untreated cells (Figure 3D), only weak fluorescent signals were detected in the intracellular compartments. This is because  $\beta$ -catenin proteins that were not sequestered by E-cadherin were tagged for degradation by the Axin·APC·GSK-3 $\beta$  protein complex. Only when E-cadherin is downregulated or functionally inactivated or Wnt signaling is turned on does  $\beta$ -catenin accumulate in the cytoplasm and subsequently translocate to the nucleus.<sup>35</sup> Since only the **T1**-treated cells showed  $\beta$ -catenin nuclear localization, it further confirms that the observed cellular responses are sequence-specific.

Consistent with the results above, cells treated with **T1**, when stained with phalloidin, which binds to the actin cytoskeleton, showed an unusual pattern where cells appeared to be elongated and crawled on top of one another (compare part H with G and I, Figure 3). This phenotype is again consistent with cells losing contact inhibition, characteristic of E-cadherin downregulation.<sup>39</sup>

Loss of E-cadherin function or expression has, in fact, been implicated in cancer progression and metastasis.<sup>46</sup> On the other hand, no noticeable changes in either cell morphology or cell contact inhibition were observed for cells treated with **T1-M3** as compared to the control. This result further corroborates the findings above.

**Cell Motility.** To further confirm that the observed antisense effect is specific to E-cadherin, we examined the effects of **T1** and **T1-M3** on cell migration. Cells were grown to near confluent ( $\sim 80\%$ ) before treating with GPNAs. After 48-h treatment (at which point cells were confluent), a scratch (“wound”) was made. A DIC image was taken ( $t = 0$ ) and cells were allowed to grow for an additional 20 h before another DIC image of the same region was taken again ( $t = 20$  h). The two images, taken at  $t = 0$  and  $t = 20$  h, for the untreated and treated cells were then compared. Inspection of the wounds taken at  $t = 0$  (Figure 4A,C,F) shows that they are similar in size for all three samples. Within 20 h the wound area of the **T1**-treated sample was nearly filled with cells, whereas that of the untreated sample or sample treated with **T1-M3** remained sparse with cells (compare part D with B and F, Figure 4). This result shows that cells treated with the perfect-match **T1** oligo migrated at a much faster rate than either the mismatch **T1-M3** or the control. The increase in cell motility is consistent with the characteristic phenotype of cells losing contact inhibition as the result of E-cadherin repression.<sup>46</sup>

(46) Katagiri, A.; Watanabe, R.; Tomita, Y. *Br. J. Cancer* **1995**, *71*, 376–379.

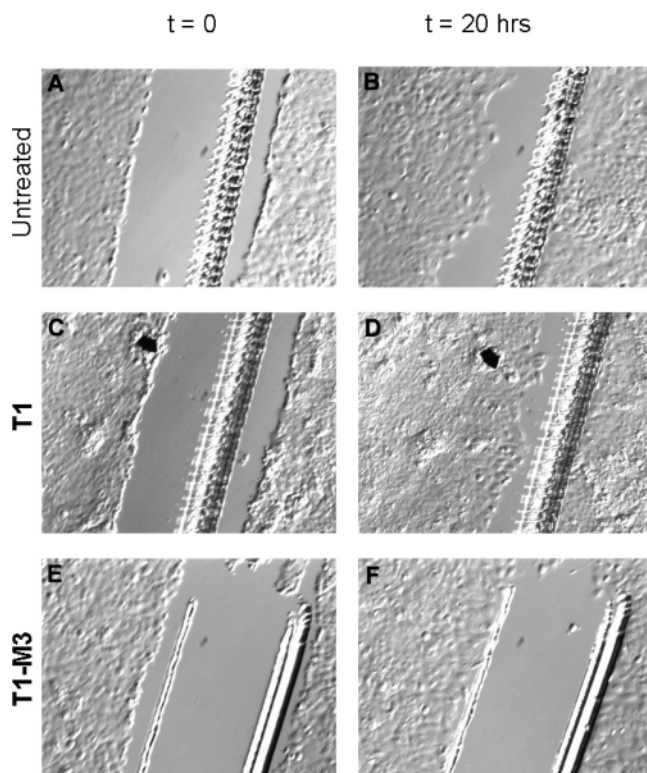


**Figure 4.** Cell motility (wound-healing) assay. Untreated A549 cells (A, B); cells treated with  $10 \mu\text{M}$  of **T1** (C, D) and **T1-M3** (E, F) GPNA. DIC (differential interference contrast) images of the wound made at  $t = 0$  (A, C, E) and at  $t = 20$  h (B, D, F).

**Mechanism of Action.** PNAs designed to bind to the RNA transcripts were thought to confer their gene silencing effects by physically blocking the ribosomal machinery, since the PNA–RNA complex cannot be recognized or degraded by RNase H.<sup>47–49</sup> A recent study by Janowski and Corey,<sup>50</sup> however, showed that PNAs designed to bind to the transcriptional start-site of human progesterone receptor A (hPR-A) and B (hPR-B) isoforms inhibit protein expression by blocking transcription. The fact that **T1** was also designed to bind to the transcriptional start-site suggests that **T1** may be operating by a similar mechanism, inhibiting E-cadherin transcription. Transcriptional inactivation may explain why **T1** is more potent than **T4**, because, in addition to blocking the translational machinery, it also blocks transcription by binding to the open-complex of the E-cadherin gene. To address this question, we performed quantitative RT-PCR on RNA samples isolated from the control cells and from cells treated with **T1** and **T1-M3**. The PCR products of E-cadherin and control gene (GADPH) for the three samples are shown in Figure 5. Comparison of the transcriptional levels of E-cadherin (inferred from the fluorescent intensity of the PCR products) of the untreated and treated samples shows that they are similar to one another. This result shows that **T1**

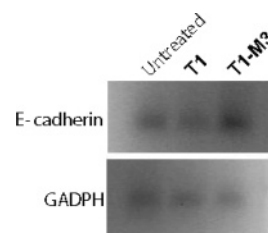


**Figure 5.** Quantitative RT-PCR of E-cadherin and GADPH gene transcript of the untreated A549 cells and cells treated with  $10 \mu\text{M}$  of **T1** and **T1-M3** GPNA oligomer for 72 h.

does not inhibit E-cadherin transcription but rather confers its silencing effect by blocking protein translation. The inability of **T1** to inhibit gene transcription could be attributed to the electrostatic interactions between the guanidinium groups of GPNA and the phosphate groups of RNA (and other biomolecules with complementary charge). Such interactions may quench **T1**, preventing it from diffusing more freely in the cytoplasm and in the nucleus as compared to the unmodified PNAs employed in Janowski and Corey's experiments.<sup>50</sup> This may also explain why a relatively high concentration of **T1** ( $1–10 \mu\text{M}$ ) is needed to induce significant antisense effects. The antisense activity of this particular class of molecules could potentially be improved if the guanidinium groups could be removed once inside the cells. This can be accomplished by using disulfide linkage to connect the guanidinium groups to the PNA backbone. A study is now underway to test this hypothesis.

**Cytotoxic Effects.** Attempt to compare the antisense activity of GPNA (**T1**) with that of the corresponding PNA–polyarginine conjugate (**T1-8R**) has also been made, since polyarginines (and related cell-penetrating peptides) are commonly used to transport PNA into cells.<sup>51</sup> Both **T1** and **T1-8R** contained the same nucleobase sequence, number of guanidinium groups (eight), and backbone configuration (D), but differed from one another in the placement of the arginine side chains, being internal for **T1** and external (at the N-terminus) for **T1-8R**. Unfortunately, such comparison could not be made due to the high toxicity of the PNA conjugate. Under identical condition ( $10 \mu\text{M}$ ), greater than 90% of the cells treated with **T1-8R** underwent apoptosis as compared to **T1** or to the control (untreated), which showed no noticeable sign of toxicity (Figure 6).

A quantitative analysis using a LIVE/DEATH cell assay showed that the cytotoxic effect increases with increasing oligomer size, being significantly more with PNA conjugates than with GNAs (Figure 7A,B). The percentage of cell death is almost double for PNA conjugates with 8 (**P8-4R**), 12 (**P12-6R**), and 16 (**P16-8R**) nucleobase- and almost triple for PNA conjugate with 20 nucleobase units (**P20-10R**) as compared to GNAs with the same sequence and number of guanidinium groups (Figure 7B). However, it should be noted that the cell density used in this experiment was relatively high, nearly confluent (80–90%) at the time of the treatment and confluent at the end of the treatment, which was 24 h later. In a similar experiment, where cells were still in the exponentially dividing state at the end of the treatment, no noticeable cytotoxic effect was observed for **P16** at  $15 \mu\text{M}$  concentration and 48-h

(47) Hanvey, J. C.; Pepper, N. J.; Bisi, J. E.; Thomson, S. A.; Cadilla, R.; Josey, J. A.; Ricca, D. J.; Hassman, C. F.; Bonham, M. A.; Au, K. G.; Carter, S. G.; Ruckenstein, D. A.; Boyd, A. L.; Noble, S. A.; Babiss, L. E. *Science* **1992**, *258*, 1481–1485.

(48) Bonham, M. A.; Brown, S.; Boyd, A. L.; Brown, P. H.; Bruckenstein, D. A.; Hanvey, J. C.; Thomson, S. A.; Pipe, A.; Hassman, F.; Bisi, J. E.; Froehler, B. C.; Matteucci, M. D.; Wagner, R. W.; Noble, S. A.; Babiss, L. E. *Nucleic Acids Res.* **1995**, *23*, 1197–1203.

(49) Knudsen, H.; Nielsen, P. E. *Nucleic Acids Res.* **1996**, *24*, 494–500.

(50) Janowski, B. A.; Kaihatsu, K.; Huffman, K. E.; Schwartz, J. C.; Ram, R.; Hardy, D.; Mendelson, C. R.; Corey, D. R. *Nat. Chem. Biol.* **2005**, *1*, 210–215.

(51) Koppellus, U.; Awasthi, S. K.; Zachar, V.; Holst, H.; Ebbesen, P.; Nielsen, P. E. *Antisense Nucleic Acids Drug Dev.* **2002**, *12*, 51–63.

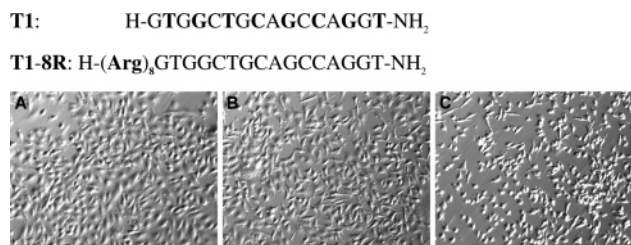


**Figure 6.** DIC images of the untreated A549 cells (A) and cells treated with 10  $\mu\text{M}$  of **T1** GPNA oligomer (B) and **T1-8R** PNA-polyarginine conjugate (C) for 24 h.

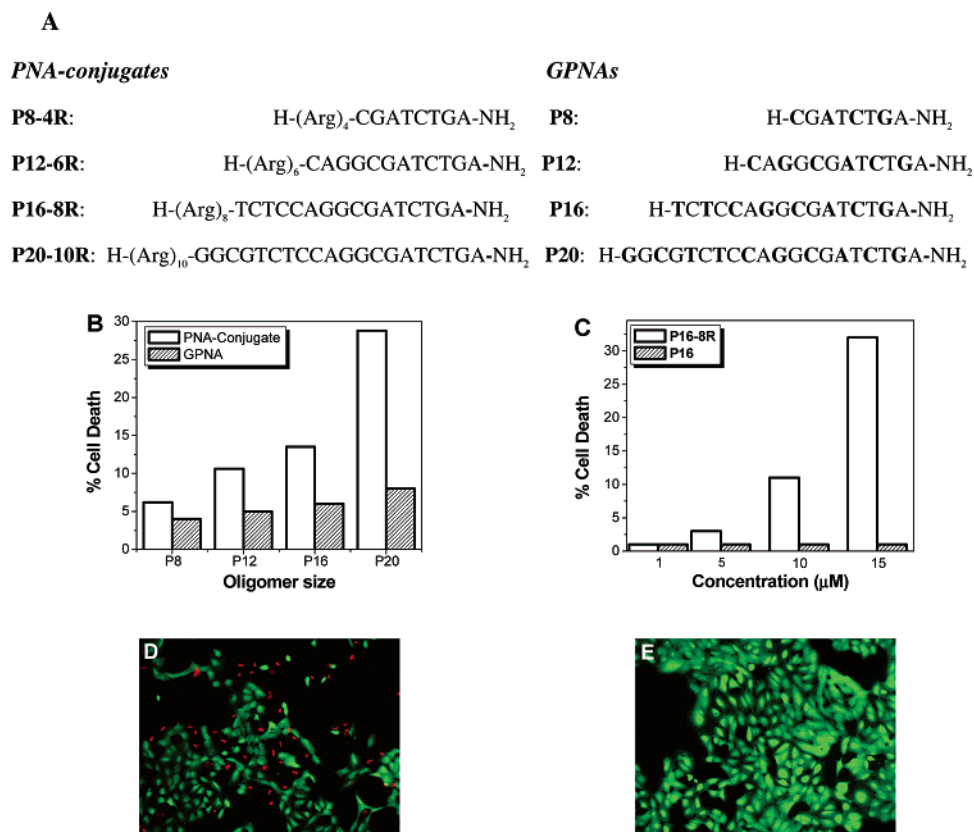


**Figure 7.** Cytotoxic effects of PNA conjugates and GPNAs. (A) The sequence of PNA conjugates and GPNAs. The configuration of arginine residues in PNA conjugates is D; bold letters denote GPNA units. (B) The effects of oligomer size on cytotoxicity. Nearly confluent (80–90%) A549 cells were treated with 10  $\mu\text{M}$  of the indicated PNA conjugates and GPNAs for 24 h and then stained with EthD-1 (dead cells) and calcein (live cells). (C) Exponentially growing A549 cells were treated with various concentrations of 16-mer PNA conjugate (**P16-8R**) and GPNA (**P16**) for 48 h and then stained with EthD-1 and calcein. Representative fluorescent images of cells treated with 15  $\mu\text{M}$  of **P16-8R** (D) and **P16** (E) for 48 h and stained with EthD-1 (red, dead cells) and calcein (green, live cells).

incubation time. On the other hand, greater than 30% cell death was observed for **P16-8R** (Figure 7C). A representative image of cells treated with **P16-8R** and **P16** after incubating with calcein AM and ethidium homodimer-1 (EthD-1) probes (components of the LIVE/DEATH assay kit) is shown in parts D and E, respectively, of Figure 7. Calcein AM is a cell-permeable, nonfluorescent dye. It only becomes fluorescent in live cells, where calcein AM is converted to calcein by the esterase enzyme, with absorption/emission at  $\sim 495/515$  nm. EthD-1, on the other hand, is not permeable to live cells. It can only enter dead cells or cells with compromised plasma membrane, with absorption/emission at  $\sim 495/634$  nm. Dead and plasma membrane-compromised cells showed EthD-1 (red) staining, while live cells showed calcein (green) staining. Comparing parts D with E of Figure 7 shows that a large proportion (30–40%) of cells treated with 15  $\mu\text{M}$  of **P16-8R** displayed EthD-1 staining, with round shape characteristic of the apoptotic cells,

while less than 1% of cells treated with **P16** displayed this same characteristic feature. The percentage of dead and plasma membrane-compromised cells shown in Figure 7B–D for PNA conjugates may be underestimated, because some of the cells may have been washed away in the washing step, since damaged cells tend to round up and detach from the cultured plates, though care was taken to minimize such loss.

It is not clear why PNA conjugates are more toxic than GPNAs, considering that they have the same nucleobase sequence, number of guanidinium groups, and backbone configuration. A survey of the literature suggests that the amphipathic nature of PNA-polyarginine conjugates may be responsible for the observed cytotoxic effects. A diverse class of antimicrobial peptides,<sup>52,53</sup> more than 500 have now been

(52) Zasloff, M. *Nature* **2002**, *415*, 389–395.

(53) Database, A. S.

identified, including the silk moth's cecropin A,<sup>54</sup> the African clawed frog's magainin 2,<sup>55</sup> and the bee's venom melittin,<sup>56</sup> are amphipathic. Most of these peptides are cationic in nature; they have a propensity to adopt compartmentalized structures, where the hydrophobic and hydrophilic amino acid residues are organized into discrete regions. These amphipathic peptides confer their antimicrobial effects by binding to and inserting themselves in the cell membrane, resulting in its permeabilization and/or disruption. Since PNA-polyarginines are also amphipathic, it is not unreasonable to suggest that a similar mechanism is operating. In this case, the hydrophilic region (polyarginine) of the conjugate interacts with the phospholipid-heads on the cell surface, while the hydrophobic domain (PNA) inserts itself into the lipid bilayers. With sufficient concentration, such interaction can perturb the normal functioning of the cell membrane that eventually results in cell death. GPNAs, on the other hand, are less toxic because they are less amphipathic in character and therefore are less likely to cause disturbance to the cell membrane.

## Conclusion

In summary, we have shown that GPNAs designed to bind to the transcriptional start-site of E-cadherin gene induce potent and sequence-specific antisense effects, with the expected molecular and cellular responses. This result is significant because it suggests the possibility of using these oligomers to assess gene function in a high-throughput fashion, since the transcriptional start-sites of many genes have already been identified<sup>37,57</sup> and GPNA oligomers could be synthesized in parallel on solid supports.<sup>58</sup> This approach could be extended to intact organisms, since no delivery system is required and it is significantly less toxic than the conventional PNA-molecular transporter design. While other methods, such as RNA interference (RNAi), have proven effective in regulating gene expression, cellular delivery and toxicity remain challenging issues.

## Experimental Section

**PNA and GPNA Oligomer Synthesis.** Boc-protected PNA monomers were purchased from Applied Biosystems (Foster City, CA), while GPNA monomers were synthesized according to established procedures.<sup>58</sup> PNA and GPNA oligomers were synthesized by standard Boc solid-phase synthesis protocols,<sup>38</sup> using cross-linked polystyrene beads functionalized with 4-methylbenzhydrylamine (MBHA) as supporting resin. An L-lysine residue was incorporated at the C-terminus of each PNA oligomer to increase water solubility. Upon completion of the last monomer coupling, PNA and GPNA oligomers were cleaved from the resin using *m*-cresol/thioanisole/TFMSA/TFA mixture (1:1:2:6) and precipitated with ether. The resulting oligomers were purified by RP-HPLC and characterized by MALDI-TOF mass spectrometry. The purified samples were dried and reconstituted with nanopure water and stored at -40 °C for long-term storage. The total strand concentrations were determined by UV absorbance at 260 nm (85 °C) using the following extinction coefficients: T = 8600 M<sup>-1</sup> cm<sup>-1</sup>, A = 13 700 M<sup>-1</sup> cm<sup>-1</sup>, C = 6600 M<sup>-1</sup> cm<sup>-1</sup>, and G = 11 700 M<sup>-1</sup> cm<sup>-1</sup>.

**Cell Culture.** A549 (lung carcinoma) and MDA-MB-435 (breast carcinoma) were obtained from the American Tissue Cell Culture (ATCC) and cultured according to the recommended protocols. Cells were either grown in cultured plates or on glass coverslips in 12-well plates alone (control) or treated with GPNA oligomers in complete medium (10% FBS) at 37 °C in 5% CO<sub>2</sub>.

**Immunocytochemistry.** Following the treatment, cells were washed three times with PBS, fixed with 4% paraformaldehyde for 15 min, permeabilized with 1% Triton-X for 15 min, and then blocked with 2% milk for 30 min before staining with primary antibody, E-cadherin (1:100) or  $\beta$ -catenin (1:100) (Santa Cruz Biotechnology), for 1 h at 37 °C. The unbound antibodies were removed, and the remaining adherent cells were washed three times with PBS and counterstained with fluorescein-isothiocyanate-conjugated antimouse IgG secondary antibody (Santa Cruz Biotechnology) for 1 h in the incubator at 37 °C and 5% CO<sub>2</sub>. Hoechst staining was added to the first wash at 1  $\mu$ g/ $\mu$ L concentration to the samples stained with E-cadherin and phalloidin, but not to the samples stained with  $\beta$ -catenin primary antibody to avoid confusing  $\beta$ -catenin nuclear localization with Hoechst (nuclear-specific) staining. For phalloidin (Santa Cruz Biotechnology) staining, cells were processed the same way as described above, but instead of staining with specific primary and then secondary antibody, permeabilized cells were stained with rhodamine-phalloidin conjugate (1:1000) (staining actin) and Hoechst (staining nucleus). Following the staining, cells were then imaged with 60 $\times$  objective using an Olympus-IX81 fluorescent microscope.

**RNA Preparation.** Total RNAs were prepared using a PARIS Protein and RNA Isolation System (Ambion) according to the instruction manual. In brief, cells were trypsinized, lysed with cell disruption buffer, mixed with ethanol, and then run through a filter cartridge provided with the kit. The cartridge was washed several times before eluting the bound RNA with elution buffer, preheated to 95 °C. The concentration of RNA was determined using the conversion 1 OD<sub>260nm</sub> = 40  $\mu$ g/mL.

**Quantitative RT-PCR.** PCR products of specific genes were amplified directly from RNA templates using a Platinum Quantitative RT-PCR ThermoScript One-Step System (Invitrogen). The 50- $\mu$ L reaction mixture contained 2X ThermoScript Reaction Mix (25  $\mu$ L), 100 ng/ $\mu$ L RNA template (1  $\mu$ L), 10  $\mu$ M forward primer (1  $\mu$ L), 10  $\mu$ M reverse primer (1  $\mu$ L), ThermoScript Plus/Platinum *Taq* Enzyme Mix (1  $\mu$ L), and autoclave distilled water (21  $\mu$ L). cDNA synthesis was performed by heating the reaction mixture in the thermocycler at 55 °C for 30 min (cDNA synthesis), and the PCR amplification steps were performed as follows: 95 °C for 5 min (1 cycle), 32 cycles of 95 °C for 30 s, 55 °C for 30 s, and 72 °C for 1 min. Primer sequence for E-cadherin: 5'-GGAAGTCAGTTCAGACTCCAGCC-3'/AGGCCTTTTGACTGTAATCACACC-3'. Primer sequence for GADPH: 5'-TGGTATCGTGAAGGACTCATGAC-3'/5'-CGACTTGCCCTTCGAGTGACCGTA-3'.

**Wound-Healing Assay.** A549 cells were cultured in the 12-well plates at ~80% confluence. Cells were incubated in complete media (control) and media containing 10  $\mu$ M of **T1** and **T1-M3** GPNA oligomer (separate treatment) for 48 h. Subsequently, the medium was removed, and cells were washed three times with PBS and refreshed with new media along with 10  $\mu$ M of **T1** and **T1-M3**. At this time the cells were confluent. A scratch was made to the confluent cells using a glass Pasteur pipet, and a DIC image was taken ( $t = 0$ ) for both the treated and untreated cells. DIC images of the same regions of the treated and untreated cells were taken again 20 h later. The images taken at  $t = 0$  and at  $t = 20$  h were compared to assess cell motility.

**Cytotoxicity Assay.** Cytotoxicity assay was performed using a LIVE/DEAD viability assay purchased from Molecular Probes. A549 cells were plated on sterile glass coverslips and allowed to grow to 80–90% confluence in cell culture incubator. The medium was removed, and cells were washed three times with PBS (to remove dead

(54) Steiner, H.; Hultmark, D.; Ensgstrom, A.; Bennich, H.; Boman, H. G. *Nature* **1981**, *292*, 246–248.

(55) Zasloff, M. *Proc. Natl. Acad. Sci. U.S.A.* **1987**, *84*, 5449–5453.

(56) Habermann, E.; Jentsch, J. *Hoppe-Seyler's Z. Physiol. Chem.* **1967**, *348*, 37–50.

(57) (DBTSS), d. o. T. S. S.

(58) Zhou, P.; Dragulescu-Andrasi, A.; Bhattacharya, B.; O'keefe, H.; Vatta, P.; Hyldig-Nielsen, J. J.; Ly, D. H. *Bioorg. Med. Chem. Lett.* **2006**, *16*, 4931–4935.



cells) and refreshed with new media. The appropriate oligomers (10  $\mu\text{M}$ ) were added and incubated for 24 h. Following the treatment, cells were washed three times with PBS and incubated with 150  $\mu\text{L}$  of the LIVE/DEAD solution, prepared by mixing 2  $\mu\text{L}$  of 2 mM EthD-1 stock solution with 0.5  $\mu\text{L}$  of calcein AM stock solution in 1 mL of PBS. The samples were incubated in the dark at room temperature for 30 min. Cells were then viewed with 20 $\times$  objective using an Olympus IX80 fluorescence microscope. The percent dead cell was calculated as followed, % dead cells = number of dead cells (EthD-1 stained)/total number of cells. A total number of 500 cells was used in each experiment, and the experiments were performed in triplicate.

**Acknowledgment.** Financial support for this work was provided by Applied Biosystems (APPLERA-LY) and National Institutes of Health (GM077261-01).

**Supporting Information Available:** Antisense effects at different **T1** concentrations and with different cell lines. This material is available free of charge via the Internet at <http://pubs.acs.org>.

JA063383V